

Status of the CPT Violating Interpretations of the LSND Signal

M. C. Gonzalez-Garcia*

Y.I.T.P., SUNY at Stony Brook, Stony Brook, NY 11794-3840, USA, and

IFIC, Universitat de València - C.S.I.C.,

Apt 22085, E-46071 València, Spain

M. Maltoni†

IFIC, Universitat de València - C.S.I.C.,

Apt 22085, E-46071 València, Spain

T. Schwetz‡

Institut für Theoretische Physik, Physik Department

Technische Universität München, James-Franck-Str., D-85748 Garching, Germany

Abstract

We study the status of the CPT violating neutrino mass spectrum which has been proposed to simultaneously accommodate the oscillation data from LSND, KamLAND, atmospheric and solar neutrino experiments, as well as the non-observation of anti-neutrino disappearance in short-baseline reactor experiments. We perform a three-generation analysis of the global data with the aim of elucidating the viability of this solution. We find no compatibility between the results of the oscillation analysis of LSND and all-but-LSND data sets below 3σ CL. Furthermore, the global data without LSND show no evidence for CPT violation: the best fit point of the all-but-LSND analysis occurs very close to a CPT conserving scenario.

*Electronic address: concha@insti.physics.sunysb.edu

†Electronic address: maltoni@ific.uv.es

‡Electronic address: schwetz@ph.tum.de

I. INTRODUCTION

The joint explanation of the oscillation signals observed in LSND [1], in solar [2, 3, 4, 5, 6, 7] and atmospheric [8, 9, 10, 11] neutrino experiments, and in the KamLAND reactor experiment [12] provides a big challenge to neutrino phenomenology. In Refs. [13, 14] it was observed that the LSND signal could be accommodated with the solar and atmospheric neutrino anomalies without enlarging the neutrino sector if CPT was violated. Once such a drastic modification of standard physics is accepted, oscillations with four independent Δm^2 are possible, two in the neutrino and two in the anti-neutrino sector. The basic realization behind these proposals is that the oscillation interpretation of the solar results involves oscillations of electron neutrinos with $\Delta m_{\odot}^2 \lesssim 10^{-4} \text{ eV}^2$ [15], while the LSND signal for short-baseline oscillations with $\Delta m_{\text{LSND}}^2 \gtrsim 10^{-1} \text{ eV}^2$ stems dominantly from anti-neutrinos ($\bar{\nu}_{\mu} \rightarrow \bar{\nu}_e$). If CPT was violated and neutrino and anti-neutrino mass spectra and mixings were different [13, 14, 16, 17, 18] both results could be made compatible in addition to the interpretation of the atmospheric neutrino data in terms of oscillations of both ν_{μ} and $\bar{\nu}_{\mu}$ with $\Delta m_{\text{atm}}^2 \sim 10^{-3} \text{ eV}^2$ [8].

In the original spectrum proposed, neutrinos had mass splittings $\Delta m_{\odot}^2 = \Delta m_{21}^2 \ll \Delta m_{31}^2 = \Delta m_{\text{atm}}^2$ to explain the solar and atmospheric observations, while for anti-neutrinos $\Delta m_{\text{atm}}^2 = \Delta \bar{m}_{21}^2 \ll \Delta \bar{m}_{31}^2 = \Delta m_{\text{LSND}}^2$. Within this spectrum the mixing angles could be adjusted to obey the relevant constraints from laboratory experiments, mainly due to the non-observation of reactor $\bar{\nu}_e$ at short distances [19, 20], and a reasonable description of the data could be achieved [18, 21, 22]. In general, stronger constraints on the possibility of CPT violation arise, once a specific source of CPT violation which involves other sectors of the theory is invoked [23]. For a summary of recent theoretical work and experimental tests see, for example, Ref. [24] and references therein.

On pure phenomenological grounds, the first test of this scenario came from the KamLAND [12] experiment since the suggested CPT-violating neutrino spectrum allowed to reconcile the solar, atmospheric and LSND anomalies, but, once the constraints from reactor experiments were imposed, no effect in KamLAND was predicted. The observation of a deficit in KamLAND at 3.5σ CL clearly disfavoured these scenarios. Furthermore, KamLAND results demonstrate that $\bar{\nu}_e$ oscillate with parameters consistent with the LMA ν_e oscillation solution of the solar anomaly. This fact by itself can be used to set constraints on the possibility of CPT violation [21, 25]. Within the present KamLAND accuracy, however, the bounds are not very strong because KamLAND data does not show a significant evidence of energy distortion.

The present situation is that the results of solar experiments in ν oscillations, together with the results from KamLAND and the bounds from other $\bar{\nu}$ reactor experiments show that both neutrinos and anti-neutrinos oscillate with $\Delta m_{\odot}^2, \Delta m_{\text{reac}}^2 \leq 10^{-3} \text{ eV}^2$. Adding this to the evidence of oscillations of both atmospheric neutrinos and anti-neutrinos with $\Delta m_{\text{atm}}^2 \sim 10^{-3} \text{ eV}^2$, leaves no room for oscillations with $\Delta m_{\text{LSND}}^2 \sim 1 \text{ eV}^2$. The obvious

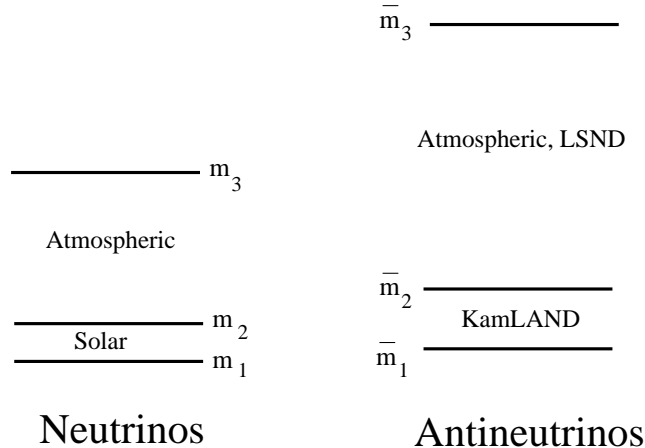


Figure 1: Post KamLAND CPT violating neutrino mass spectrum proposed in Ref. [17].

conclusion then is that CPT violation can no-longer explain LSND and perfectly fit all other data [21].

This conclusion relies strongly on the fact that atmospheric oscillations have been observed for both neutrinos and anti-neutrinos with the same Δm_{atm}^2 . However atmospheric neutrino experiments do not distinguish neutrinos from anti-neutrinos, and neutrinos contribute more than anti-neutrinos to the event rates by a factor $\sim 4-2$ (the factor decreases for higher energies). Based on this fact, in Ref. [17] an alternative CPT-violating spectrum was proposed as shown in Fig. 1.¹ In this scheme only atmospheric neutrinos oscillate with Δm_{atm}^2 and give most of the contribution to the observed zenith angular dependence of the deficit of μ -like events. Atmospheric $\bar{\nu}_\mu$ dominantly oscillate with Δm_{LSND}^2 which leads to an almost constant (energy and angular independent) suppression of the corresponding events. For low $\bar{\nu}_\mu$ energies oscillations with Δm_{reac}^2 can also be a source of zenith-angular dependence. The claim in Ref. [17] was that altogether this suffices to give a good description of the atmospheric data such that the scheme in Fig. 1 can still be a viable solution to all the neutrino puzzles. This conclusion was contradicted in Ref. [21] by an analysis of atmospheric and K2K data. However, according to the authors in Ref. [17] an important point to their conclusion was the consideration of the full 3ν and $3\bar{\nu}$ oscillations, while the analysis in Ref. [21] was made on the basis of a $2\nu+2\bar{\nu}$ approximation.

In this article we determine the status of the CPT violating scenario in Fig. 1 as explanation to the existing neutrino anomalies. In order to do this, we perform a three-generation global analysis of the solar, atmospheric, reactor, and long-baseline (LBL) data, and compare the allowed parameter regions from this analysis to the ones required to explain the LSND data. We find that no consistency between the parameters determined by the analyses

¹ This possibility was also discussed in the first version of Ref. [21].

of both data sets appears below 3σ CL.

II. NOTATION AND DATA INPUTS

In what follows we label the states as in Fig. 1 with $\Delta m_{ij}^2 = m_i^2 - m_j^2$ and $\Delta \bar{m}_{ij}^2 = \bar{m}_i^2 - \bar{m}_j^2$. We denote by U and \bar{U} the corresponding neutrino and anti-neutrino mixing matrix [26] which we chose to parametrize as [27]

$$U = \begin{pmatrix} c_{13}c_{12} & s_{12}c_{13} & s_{13} \\ -s_{12}c_{23} - s_{23}s_{13}c_{12} & c_{23}c_{12} - s_{23}s_{13}s_{12} & s_{23}c_{13} \\ s_{23}s_{12} - s_{13}c_{23}c_{12} & -s_{23}c_{12} - s_{13}s_{12}c_{23} & c_{23}c_{13} \end{pmatrix}, \quad (1)$$

where $c_{ij} \equiv \cos \theta_{ij}$ and $s_{ij} \equiv \sin \theta_{ij}$ and with ‘‘over-bar’’ for the corresponding anti-neutrino mixing. In writing Eq. (1) we take into account that for our following description it is correct and sufficient to set all the CP phases to zero.

In the anti-neutrino sector the reactor experiments [12, 19, 20] provide information on the $\bar{\nu}_e$ survival probability:

$$\begin{aligned} P_{ee}^{\text{reac}} &= 1 - \bar{c}_{13}^4 \sin^2 2\bar{\theta}_{12} \sin^2 \left(\frac{\Delta \bar{m}_{21}^2 L}{4E} \right) \\ &\quad - \sin^2 2\bar{\theta}_{13} \left[\bar{c}_{12}^2 \sin^2 \left(\frac{\Delta \bar{m}_{31}^2 L}{4E} \right) + \bar{s}_{12}^2 \sin^2 \left(\frac{\Delta \bar{m}_{32}^2 L}{4E} \right) \right] \\ &\simeq \begin{cases} 1 - \sin^2 2\bar{\theta}_{13} \sin^2 \left(\frac{\Delta \bar{m}_{31}^2 L}{4E} \right) & \text{for } \Delta \bar{m}_{21}^2 L/E \ll 1 \\ \bar{s}_{13}^4 + \bar{c}_{13}^4 \left[1 - \sin^2 2\bar{\theta}_{12} \sin^2 \left(\frac{\Delta \bar{m}_{21}^2 L}{4E} \right) \right] & \text{for } \Delta \bar{m}_{31}^2 L/E \gg 1 \end{cases} \end{aligned} \quad (2)$$

In our analysis we include the results from the KamLAND [12], Bugey [20] and CHOOZ [19] reactor experiments. For KamLAND we include information on the observed anti-neutrino spectrum which accounts for a total of 13 data points. Details of our calculations and statistical treatment of KamLAND data can be found in Ref. [28]. For reactor experiments performed at short-baselines we include the constraints from Bugey [20] and CHOOZ [19] which are the most relevant for $\Delta \bar{m}^2 \gtrsim 0.03 \text{ eV}^2$ and $0.03 \text{ eV}^2 \gtrsim \Delta \bar{m}^2 \gtrsim 10^{-3} \text{ eV}^2$, respectively. In our analysis of the CHOOZ data we include their energy binned data which corresponds to 14 data points (7-bin positron spectra from both reactors, Table 4 in Ref. [19]) with one constrained normalization parameter. For the analysis of Bugey data we use a total of 60 data points given in Fig. 17 of Ref. [20], where the ratio of the observed number of events to the one expected for no oscillations is shown for the three distances 15 m, 40 m, and 90 m. For technical details of our Bugey analysis see Ref. [29].

In the scheme under consideration the probability associated with the $\bar{\nu}_\mu \rightarrow \bar{\nu}_e$ signal in

LSND is given by

$$P_{\text{LSND}} \equiv \sin^2 2\theta_{\text{LSND}} \sin^2 \left(\frac{\Delta m_{\text{LSND}}^2 L}{4E} \right) = \bar{s}_{23}^2 \sin^2 2\bar{\theta}_{13} \sin^2 \left(\frac{\Delta \bar{m}_{31}^2 L}{4E} \right), \quad (3)$$

where we have neglected terms proportional to $\Delta \bar{m}_{21}^2$ which are irrelevant for LSND distances and energies. In Eq. (3) we have introduced the notation

$$\Delta m_{\text{LSND}}^2 = \Delta \bar{m}_{31}^2, \quad \sin^2 2\theta_{\text{LSND}} = \bar{s}_{23}^2 \sin^2 2\bar{\theta}_{13} \quad (4)$$

which we will use in the presentation of our results. To include LSND we use the results of Ref. [30], based only on the decay-at-rest anti-neutrino data sample. The χ_{LSND}^2 is derived from a likelihood function obtained from an event-by-event analysis of the data [30]. LSND has also studied the neutrino channel $\nu_\mu \rightarrow \nu_e$ from decay-in-flight events, leading to results consistent with the ones from the anti-neutrino data sample. However, the signal in the neutrino channel is not strong, and hence, provides no statistically significant information about the CPT scenario. Therefore, we do not include it in the analysis.

For the neutrino sector we use information from solar neutrino experiments and the K2K [31] LBL experiment. For the solar neutrino analysis we use 80 data points. We include the two measured radiochemical rates, from the chlorine [4] and the gallium [5, 6, 7] experiments, the 44 zenith-spectral energy bins of the electron neutrino scattering signal measured by the SK collaboration [3], and the 34 day-night spectral energy bins measured with the SNO [2] detector. We take account of the BP00 [32] predicted fluxes and uncertainties for all solar neutrino sources except for the ^8B flux which we treat as a free parameter. For the relevant cases oscillations with Δm_{31}^2 are average out for solar neutrinos and the survival probability takes the form:

$$P_{ee}^{3\nu, \text{sol}} = s_{13}^4 + c_{13}^4 P_{ee}^{2\nu, \text{sol}}(\Delta m_{21}^2, \theta_{12}), \quad (5)$$

where $P_{ee}^{2\nu, \text{sol}}(\Delta m_{21}^2, \theta_{12})$ is the survival probability for 2ν mixing obtained with the modified matter density $N_e \rightarrow c_{13}^2 N_e$.

The results of the analysis of the solar neutrino data [15] imply that Δm_{21}^2 has to be small enough to be irrelevant for the K2K baseline and energy, and the ν_μ survival probability at K2K is

$$P_{\mu\mu}^{\text{K2K}} = 1 - 4 (s_{23}^4 s_{13}^2 c_{13}^2 + c_{13}^2 s_{23}^2 c_{23}^2) \sin^2 \left(\frac{\Delta m_{32}^2 L}{4E} \right). \quad (6)$$

In the analysis of K2K we include the data on the normalization and shape of the spectrum of single-ring μ -like events as a function of the reconstructed neutrino energy. The total sample corresponds to 29 events [31]. We bin the data in five 0.5 GeV bins with $0 < E_{\text{rec}} < 2.5$ plus one bin containing all events above 2.5 GeV. The details of the analysis can be found in Ref. [33].

Finally, the analysis of atmospheric neutrino data involves oscillations of both neutrinos and anti-neutrinos, and, in the framework of $3\nu+3\bar{\nu}$ mixing, matter effects become relevant.

We solve numerically the evolution equations for neutrinos and anti-neutrinos in order to obtain the corresponding oscillation probabilities for both e and μ flavours. In our calculations, we use the PREM model of the Earth [34] matter density profile. We include in our analysis all the contained events from the 1489 SK data set [8], as well as the upward-going neutrino-induced muon fluxes from both SK and the MACRO detector [10]. This amounts for a total of 65 data points. More technical descriptions of our simulation and statistical analysis can be found in Ref. [35].

III. RESULTS

Our basic approach to test the status of the scheme in Fig. 1 as a possible explanation of the LSND anomaly together with all other neutrino and anti-neutrino oscillation data is as follows. First, we perform a global analysis of all the relevant data, but leaving out LSND data. The goal of this analysis is to obtain the allowed ranges of parameters Δm_{LSND}^2 and $\sin^2 2\theta_{\text{LSND}}$ as defined in Eq. (4) from this all-but-LSND data set. We then compare these allowed regions to the corresponding allowed parameter region from LSND, and quantify at which CL both regions become compatible.

In this approach we start by defining the most general χ^2 for the all-but-LSND data set:

$$\begin{aligned} \chi_{\text{all-but-LSND}}^2(\Delta m_{21}^2, \Delta m_{31}^2, \theta_{12}, \theta_{23}, \theta_{13} | \Delta \bar{m}_{21}^2, \Delta \bar{m}_{31}^2, \bar{\theta}_{12}, \bar{\theta}_{23}, \bar{\theta}_{13}) &= \chi_{\text{sol}}^2(\Delta m_{21}^2, \theta_{12}, \theta_{13}) \\ &+ \chi_{\text{K2K}}^2(\Delta m_{31}^2, \theta_{23}, \theta_{13}) + \chi_{\text{Bugey+CHOOZ+KLAND}}^2(\Delta \bar{m}_{21}^2, \Delta \bar{m}_{31}^2, \bar{\theta}_{12}, \bar{\theta}_{13}) \\ &+ \chi_{\text{ATM}}^2(\Delta m_{21}^2, \Delta m_{31}^2, \theta_{12}, \theta_{23}, \theta_{13} | \Delta \bar{m}_{21}^2, \Delta \bar{m}_{31}^2, \bar{\theta}_{12}, \bar{\theta}_{23}, \bar{\theta}_{13}). \end{aligned} \quad (7)$$

Notice that in this comparison we have not included the constraints from the non-observation of $\bar{\nu}_\mu \rightarrow \bar{\nu}_e$ transitions at KARMEN [36], which, by themselves, disfavour part of the LSND allowed parameter region. The reason for this omission is that we want to test the status of the CPT interpretation of the LSND signal using data independent of the ‘‘tension’’ between LSND and KARMEN results [30].

We first focus on the parameters Δm_{21}^2 and θ_{12} . These parameters are dominantly determined by solar neutrino data, which for any θ_{13} prefer values of Δm_{21}^2 well below the sensitivity of atmospheric neutrino data. Therefore, solar data is mostly important to enforce the ‘‘decoupling’’ of the Δm_{21}^2 oscillations from the problem. In other words, the atmospheric neutrino analysis can be made without any loss of generality, in the standard hierarchical approximation for neutrinos, neglecting the effect Δm_{21}^2 but keeping the generic- 3ν dependence on θ_{13} . Notice that, unlike in the CPT conserving case, in the relevant ranges of mass differences, θ_{13} is not bounded by any ‘‘terrestrial’’ experiment. The dominant source of information on θ_{13} is atmospheric data (and less important also solar data), and for this reason we consistently take into account this parameter in our analysis. Thus, after the marginalization over Δm_{21}^2 and θ_{12} Eq. (7) takes the form

$$\begin{aligned}
\chi_{\text{all-but-LSND}}^2(\Delta m_{31}^2, \theta_{23}, \theta_{13} | \Delta \bar{m}_{21}^2, \Delta \bar{m}_{31}^2, \bar{\theta}_{12}, \bar{\theta}_{23}, \bar{\theta}_{13}) &= \chi_{\text{sol,marg12}}^2(\theta_{13}) \\
&+ \chi_{\text{K2K}}^2(\Delta m_{31}^2, \theta_{23}, \theta_{13}) + \chi_{\text{Bugey+CHOOZ+KLAND}}^2(\Delta \bar{m}_{21}^2, \Delta \bar{m}_{31}^2, \bar{\theta}_{12}, \bar{\theta}_{13}) \\
&+ \chi_{\text{ATM}}^2(\Delta m_{31}^2, \theta_{23}, \theta_{13} | \Delta \bar{m}_{21}^2, \Delta \bar{m}_{31}^2, \bar{\theta}_{12}, \bar{\theta}_{23}, \bar{\theta}_{13}). \quad (8)
\end{aligned}$$

Let us now discuss the information on $\Delta \bar{m}_{21}^2$ from reactor experiments. The observation of the $\bar{\nu}_e$ deficit in KamLAND favours $\Delta \bar{m}_{21}^2$ values near the best fit $\Delta \bar{m}_{21}^2 = 7 \times 10^{-5} \text{ eV}^2$. For such small values oscillations with $\Delta \bar{m}_{21}^2$ have no effect for atmospheric neutrinos. Therefore, we will start by studying the case $\Delta \bar{m}_{21}^2 \leq 10^{-4} \text{ eV}^2$ in Secs. III A and III B. We will relax this assumption in Sec. III C, where we investigate also a possible effect of larger values of $\Delta \bar{m}_{21}^2$. Notice also, that the case of small $\Delta \bar{m}_{21}^2$ is continuously connected to the CPT conserving scenario since it allows for CPT conservation in the ‘‘12’’ sector. For $\Delta \bar{m}_{21}^2 \leq 10^{-4} \text{ eV}^2$, one can easily marginalize over $\Delta \bar{m}_{21}^2$ and $\bar{\theta}_{12}$ and Eq. (8) further simplifies to

$$\begin{aligned}
\chi_{\text{all-but-LSND}}^2(\Delta m_{31}^2, \theta_{23}, \theta_{13} | \Delta \bar{m}_{31}^2, \bar{\theta}_{23}, \bar{\theta}_{13}) &= \chi_{\text{sol,marg12}}^2(\theta_{13}) + \chi_{\text{K2K}}^2(\Delta m_{31}^2, \theta_{23}, \theta_{13}) \\
&+ \chi_{\text{Bugey+CHOOZ+KLAND,marg12}}^2(\Delta \bar{m}_{31}^2, \bar{\theta}_{13}) + \chi_{\text{ATM}}^2(\Delta m_{31}^2, \theta_{23}, \theta_{13} | \Delta \bar{m}_{31}^2, \bar{\theta}_{23}, \bar{\theta}_{13}). \quad (9)
\end{aligned}$$

Finally, we notice that for any value $\Delta \bar{m}_{31}^2 \gtrsim 10^{-3} \text{ eV}^2$ the results from CHOOZ or, for larger values of $\Delta \bar{m}_{31}^2$, from Bugey, imply a strong limit on $\sin^2 2\bar{\theta}_{13}$, and in order to obtain the $\bar{\nu}_e$ disappearance observed in KamLAND $\bar{\theta}_{13}$ has to be small. Within this bound the results of the atmospheric neutrino analysis are almost independent of the exact value of $\bar{\theta}_{13}$ and this parameter can be effectively set to zero in χ_{ATM}^2 without any loss of generality.

A. Analysis of all-but-LSND data

Using all the data described above except from the LSND experiment we find the following all-but-LSND best fit point:

$$\begin{aligned}
\Delta m_{31}^2 &= 2.8 \times 10^{-3} \text{ eV}^2 & \Delta \bar{m}_{31}^2 &= 2 \times 10^{-3} \text{ eV}^2 \\
\Delta m_{21}^2 &= 5.8 \times 10^{-5} \text{ eV}^2 & \Delta \bar{m}_{21}^2 &= 7.1 \times 10^{-5} \text{ eV}^2 \\
s_{23}^2 &= 0.5 & \bar{s}_{23}^2 &= 0.5 \\
s_{13}^2 &= 0 & \bar{s}_{13}^2 &= 0.01 \\
s_{12}^2 &= 0.31 & \bar{s}_{12}^2 &= 0.34
\end{aligned} \quad (10)$$

with $\chi_{\text{all-but-LSND,min}}^2 = 186.5$ for $238 - 11 = 227$ dof.² This can be directly compared to the corresponding analysis in the CPT conserving scenario:

$$\begin{aligned}
\Delta m_{31}^2 &= \Delta \bar{m}_{31}^2 = 2.6 \times 10^{-3} \text{ eV}^2 \\
\Delta m_{21}^2 &= \Delta \bar{m}_{21}^2 = 7.1 \times 10^{-5} \text{ eV}^2
\end{aligned}$$

² The 10 neutrino parameters shown in Eq. (10) plus the free solar ^8B flux give a total of 11 fitted parameters.

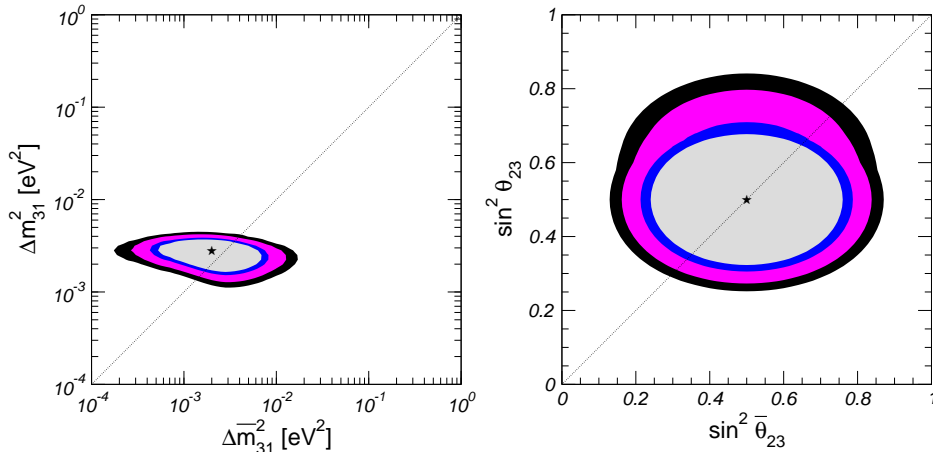


Figure 2: Allowed regions for the largest neutrino and anti-neutrino mass splittings Δm_{31}^2 and $\Delta \bar{m}_{31}^2$ and the mixing angles θ_{23} and $\bar{\theta}_{23}$ (after marginalization with respect to the undisplayed parameters) in the CPT violating scenario of Fig. 1 with $\Delta m_{21}^2, \Delta \bar{m}_{21}^2 \leq 10^{-4} \text{ eV}^2$ (see text for details). The different contours correspond to the two-dimensional allowed regions at 90%, 95%, 99% and 3σ CL. The best fit point is marked with a star. The thin lines correspond to CPT conservation.

$$\begin{aligned}
 s_{23}^2 &= \bar{s}_{23}^2 = 0.5 \\
 s_{13}^2 &= \bar{s}_{13}^2 = 0.009 \\
 s_{12}^2 &= \bar{s}_{12}^2 = 0.31
 \end{aligned}
 \tag{11}$$

with $\chi_{\text{all-but-LSND, min}}^2 = 187$ for $238 - 6 = 232$ dof. We conclude that, allowing for different mass and mixing parameters for neutrinos and anti-neutrinos, all-but-LSND data choose a best fit point very close to CPT conservation and maximal 23 mixing.

Next we illustrate the amount of CPT violation which is still viable. In order to do so we plot in Fig. 2 the allowed regions for the largest neutrino and anti-neutrino mass splittings Δm_{31}^2 and $\Delta \bar{m}_{31}^2$ and the mixing angles θ_{23} and $\bar{\theta}_{23}$ (after marginalization with respect to all the undisplayed parameters). The different contours correspond to regions allowed at 90%, 95%, 99% and 3σ CL for 2 dof ($\Delta\chi^2 = 4.61, 5.99, 9.21, 11.83$, respectively). The regions are larger for anti-neutrino parameters as a consequence of their smaller contribution to the atmospheric event rates. Our results for the allowed regions for the largest neutrino and anti-neutrino mass splittings show good qualitative agreement with the 2ν analyses of Refs. [8, 21], although, as expected, the introduction of the 3ν mixing and the reactor data leads to some quantitative differences in the size of allowed regions.

From our results shown in Eqs. (10), (11) and in Fig. 2 we conclude that current global neutrino oscillation data excluding LSND show no evidence for CPT violation, since the best fit point is very close to a CPT conserving scenario. However, from present data a

sizable amount of CPT violation by neutrino parameters is allowed (compared *e.g.* to the strong limits existing on the $K - \bar{K}$ mass difference [27]). We note that it will be possible to significantly improve the limits on CPT violation in the neutrino sector by future experiments such as neutrino factories, see for example Ref. [37].

Concerning LSND, we find that values of $\Delta\bar{m}_{31}^2 = \Delta\bar{m}_{\text{LSND}}^2$ large enough to fit the LSND result do not appear as part of the 3σ CL allowed region of the all-but-LSND analysis which is bounded to $\Delta\bar{m}_{31}^2 < 1.6 \times 10^{-2} \text{ eV}^2$. The upper bound on $\Delta\bar{m}_{31}^2$ is determined by atmospheric neutrino data (and slightly strengthened by the reactor constraints). To illustrate the physics behind this result we show in Fig. 3 the zenith-angle distributions of various atmospheric data samples for “Point A” with the following parameter values: $\Delta m_{31}^2 = 2.5 \times 10^{-3} \text{ eV}^2$, $\Delta\bar{m}_{31}^2 = 0.9 \text{ eV}^2$, $s_{23}^2 = \bar{s}_{23}^2 = 0.5$, $s_{13}^2 = 0.05$, $\bar{s}_{13}^2 = 0.005$, $\Delta m_{21}^2 \lesssim 10^{-4} \text{ eV}^2$, and $\Delta\bar{m}_{21}^2 \lesssim 10^{-4} \text{ eV}^2$. This point has been chosen to be compatible with the LSND result while keeping an optimized $\chi_{\text{all-but-LSND}}^2$. As seen in the figure this point fails in reproducing the up-down asymmetry of multi-GeV muons as a consequence of the angular-independence in the deficit of the anti-neutrino events. Furthermore, it predicts a too large deficit of up-going muon events near the horizon since $\bar{\nu}_\mu$ oscillations with $\Delta\bar{m}_{31}^2 = 0.9 \text{ eV}^2$ lead to the disappearance of $\bar{\nu}_\mu$ ’s even at those higher energies and shorter distances. For up-going muons the contribution from anti-neutrino events is only half of that from neutrino events. As a consequence this data sample is most sensitive to the anti-neutrino oscillation parameters. Both effects, the wash out of the up-down asymmetry and the deficit of horizontally arriving up-going muons, contribute in comparable amount to the statistical disfavouring of the CPT violating scenario.

B. Comparison of the all-but-LSND and the LSND data sets

It is clear from these results that the CPT violation scenario cannot give a good description of the LSND data and simultaneously fit all-but-LSND results. The quantification of this statement is displayed in Fig. 4 where we show the allowed regions in the $(\Delta\bar{m}_{31}^2 = \Delta m_{\text{LSND}}^2, \sin^2 2\theta_{\text{LSND}})$ plane required to explain the LSND signal together with the corresponding allowed regions from our global analysis of all-but-LSND data.

Fig. 4 illustrates that below 3σ CL there is no overlap between the allowed region of the LSND analysis and the all-but-LSND one, and that for this last one the region is restricted to $\Delta\bar{m}_{31}^2 = \Delta m_{\text{LSND}}^2 < 0.02 \text{ eV}^2$. At higher CL values of $\Delta\bar{m}_{31}^2 \sim \mathcal{O}(\text{eV}^2)$ become allowed – as determined mainly by the constraints from Bugey – and an agreement becomes possible. We find that in the neighbourhood of $\Delta\bar{m}_{31}^2 = \Delta m_{\text{LSND}}^2 = 0.9 \text{ eV}^2$ and $\sin^2 2\theta_{\text{LSND}} = 0.01$ the LSND and the all-but-LSND allowed regions start having some marginal agreement slightly above 3σ CL (at $\Delta\chi^2 = 12.2$). A less fine-tuned agreement appears at 3.3σ CL ($\Delta\chi^2 \sim 14$) for $\Delta\bar{m}_{31}^2 = \Delta m_{\text{LSND}}^2 \gtrsim 0.5 \text{ eV}^2$ and $\sin^2 2\theta_{\text{LSND}} \lesssim 0.01$.

Alternatively the quality of the joint description of LSND and all the other data can be

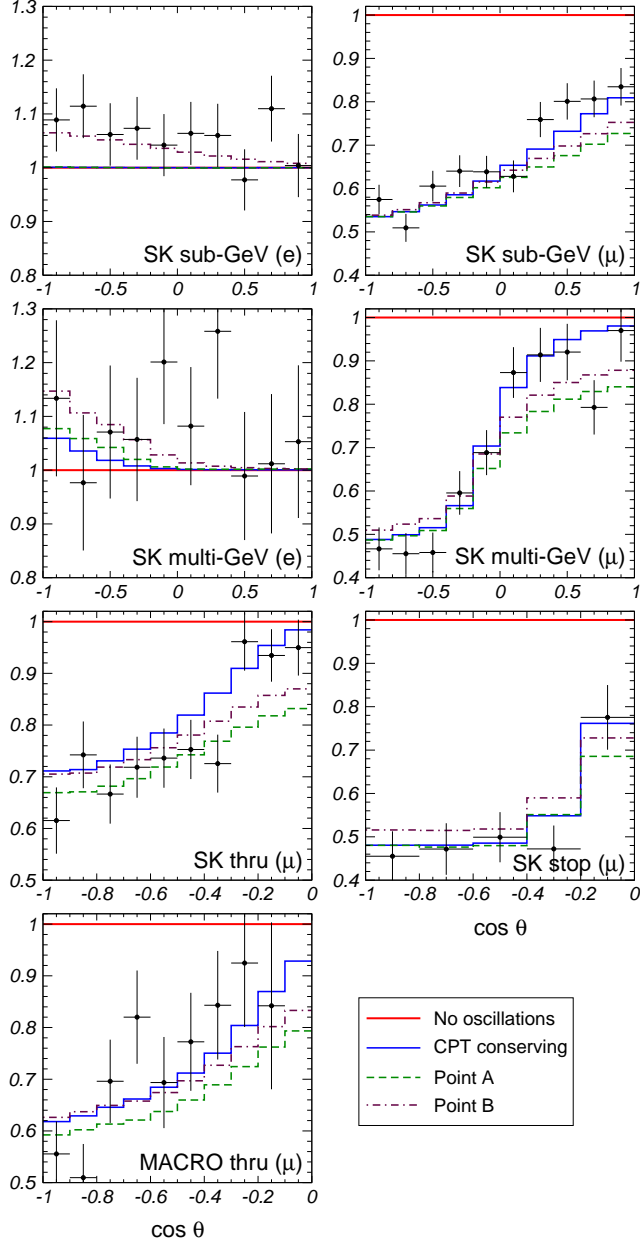


Figure 3: Zenith-angle distributions (normalized to the no-oscillation prediction) for the Super-Kamiokande e -like and μ -like contained events, for the Super-Kamiokande stopping and through-going muon events and for Macro up-going muons. The full line gives the distribution for the best fit of $\nu_\mu \rightarrow \nu_\tau$ oscillations and CPT conservation: $\Delta m_{31}^2 = \Delta \bar{m}_{31}^2 = 2.6 \times 10^{-3} \text{ eV}^2$, $s_{23}^2 = \bar{s}_{23}^2 = 0.5$, $s_{13}^2 = \bar{s}_{13}^2 = 0$, and $\Delta m_{21}^2 = \Delta \bar{m}_{21}^2 \lesssim 10^{-4} \text{ eV}^2$. The lines label as “Point A” and “Point B” are the expected distributions for typical LSND-compatible CPT violating cases with the following parameter values: Point A: $\Delta m_{31}^2 = 2.5 \times 10^{-3} \text{ eV}^2$, $\Delta \bar{m}_{31}^2 = 0.9 \text{ eV}^2$, $s_{23}^2 = \bar{s}_{23}^2 = 0.5$, $s_{13}^2 = 0.05$, $\bar{s}_{13}^2 = 0.005$, $\Delta m_{21}^2 \lesssim 10^{-4} \text{ eV}^2$, and $\Delta \bar{m}_{21}^2 \lesssim 10^{-4} \text{ eV}^2$; Point B: $\Delta m_{31}^2 = 2.5 \times 10^{-3} \text{ eV}^2$, $\Delta \bar{m}_{31}^2 = \mathcal{O}(\text{eV}^2)$, $s_{23}^2 = 0.5$, $\bar{s}_{23}^2 = 0.25$, $s_{13}^2 = 0.05$, $\bar{s}_{13}^2 = 0.005$, $\Delta m_{21}^2 \lesssim 10^{-4} \text{ eV}^2$, $\Delta \bar{m}_{21}^2 = 5 \times 10^{-4} \text{ eV}^2$, and $\bar{s}_{12}^2 = 0.75$.

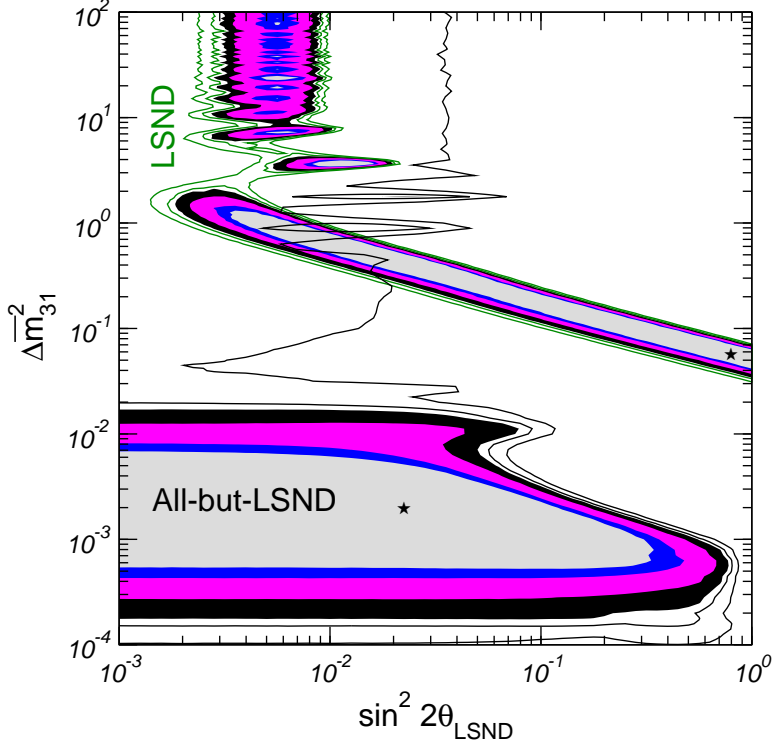


Figure 4: 90%, 95%, 99%, and 3σ CL allowed regions (filled) in the $(\Delta\bar{m}_{31}^2 = \Delta m_{\text{LSND}}^2, \sin^2 2\theta_{\text{LSND}})$ plane required to explain the LSND signal together with the corresponding allowed regions from our global analysis of all-but-LSND data. The contour lines correspond to $\Delta\chi^2 = 13$ and 16 (3.2σ and 3.6σ , respectively).

evaluated by performing a global fit based on the total χ^2 -function $\chi_{\text{tot}}^2 = \chi_{\text{all-but-LSND}}^2 + \chi_{\text{LSND}}^2$, and applying a goodness-of-fit test. The best fit point of the global analysis is $\sin^2 2\theta_{\text{LSND}} = 6.3 \times 10^{-3}$ and $\Delta\bar{m}_{31}^2 = 0.89 \text{ eV}^2$ with $\chi_{\text{tot},\text{min}}^2 = 200.9$. In the following we will use the so-called parameter goodness-of-fit [38, 39], which is particularly suitable to test the compatibility of independent data sets. Applying this method to the present case we consider the statistic

$$\begin{aligned} \bar{\chi}^2 &\equiv \chi_{\text{tot},\text{min}}^2 - \chi_{\text{all-but-LSND},\text{min}}^2 - \chi_{\text{LSND},\text{min}}^2 \\ &= \Delta\chi_{\text{all-but-LSND}}^2(\text{b.f.}) + \Delta\chi_{\text{LSND}}^2(\text{b.f.}), \end{aligned} \quad (12)$$

where b.f. denotes the global best fit point. The $\bar{\chi}^2$ of Eq. (12) has to be evaluated for 2 dof, corresponding to the two parameters $\sin^2 2\theta_{\text{LSND}}$ and $\Delta\bar{m}_{31}^2 = \Delta m_{\text{LSND}}^2$ coupling the two data sets: all-but-LSND and LSND (see Ref. [39] for details about the parameter goodness-of-fit). From $\Delta\chi_{\text{all-but-LSND}}^2 = 12.7$ and $\Delta\chi_{\text{LSND}}^2 = 1.7$ we obtain $\bar{\chi}^2 = 14.4$ leading to the marginal parameter goodness-of-fit of 7.5×10^{-4} .

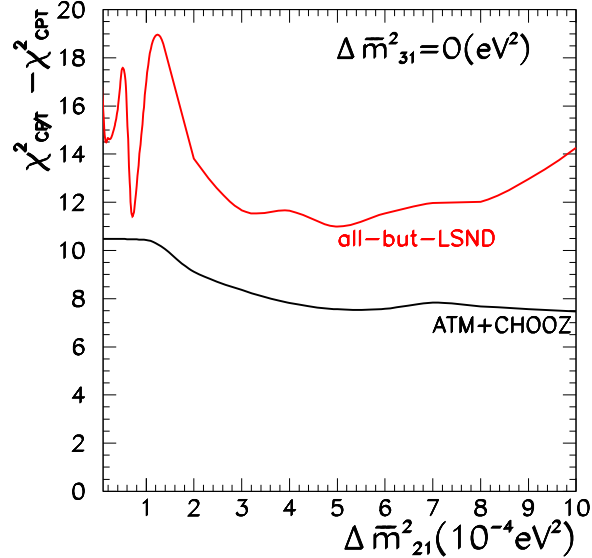


Figure 5: $\Delta\chi^2 = \chi_{\min, \text{CPT}}^2 - \chi_{\min, \text{CPT}}^2$ as a function of $\Delta\bar{m}_{21}^2$ from the analysis of atmospheric+CHOOZ data (lower line) and from all-but-LSND (upper line) data (see text for details).

C. The effect of large $\Delta\bar{m}_{21}^2$

Finally, we study whether the conclusions of the previous subsections could be affected by allowing for larger values of $\Delta\bar{m}_{21}^2$, such that its effect can show up in the atmospheric neutrino data and improve the quality of the fit as suggested in Ref. [17]. In Fig. 5 we show the dependence on $\Delta\bar{m}_{21}^2$ of the χ^2 obtained for the analysis of atmospheric and CHOOZ data, and for all-but-LSND data. In each curve we have marginalized with respect to the undisplayed variables subject to the condition $\Delta\bar{m}_{31}^2 \gtrsim 1 \text{ eV}^2$. For the sake of normalization we have subtracted in each case the corresponding $\chi_{\min, \text{CPT}}^2$ for the CPT conserving scenario.

The figure shows that, indeed, considering only atmospheric+CHOOZ data there is an improvement (although mild) in the quality of the fit due to the effect of oscillations with larger values of $\Delta\bar{m}_{21}^2$. To illustrate this result we show in Fig. 3 the zenith-angle distributions of various atmospheric data samples for “Point B”, which gives the lowest $\chi_{\text{all-but-LSND}}^2$ for a larger value of $\Delta\bar{m}_{21}^2$: $\Delta m_{31}^2 = 2.5 \times 10^{-3} \text{ eV}^2$, $\Delta\bar{m}_{31}^2 = \mathcal{O}(\text{eV}^2)$, $s_{23}^2 = 0.5$, $\bar{s}_{23}^2 = 0.25$, $s_{13}^2 = 0.05$, $\bar{s}_{13}^2 = 0.005$, $\Delta m_{21}^2 \lesssim 10^{-4} \text{ eV}^2$, $\Delta\bar{m}_{21}^2 = 5 \times 10^{-4} \text{ eV}^2$, and $\bar{s}_{12}^2 = 0.75$. The figure shows that the main effect of $\Delta\bar{m}_{21}^2$ oscillations is to increase the number of contained e -like events, in particular sub-GeV [40, 41], improving the fit for those events. However, the two main sources of discrepancy in the atmospheric fit in these scenarios – the small up-down asymmetry for multi-GeV muon-like events and the deficit of horizontally arriving up-going muons – remain a problem even when atmospheric anti-neutrino oscillations with the two relevant wavelengths are included. In other words, our results show that atmospheric neutrino data is precise enough to be sensitive to the anti-neutrino oscillation parameters, and it cannot be well described by a combination of neutrino oscillations with $\Delta m_{31}^2 \simeq 3 \times$

10^{-3} eV^2 and anti-neutrino two-wavelength oscillations with $\Delta\bar{m}_{31}^2 \sim \mathcal{O}(\text{eV}^2)$ and $\Delta\bar{m}_{21}^2 \sim \text{few } 10^{-4} \text{ eV}^2$.

The net effect in the global all-but-LSND analysis is that the improvement in the atmospheric fit is not enough to make the scenarios viable because it does not fully overcome the preference of smaller $\Delta\bar{m}_{21}^2$ in KamLAND (even within their present limited statistics) as illustrated in the all-but-LSND curve in Fig. 5. The local minimum at $\Delta\bar{m}_{21}^2 = 7.1 \times 10^{-5} \text{ eV}^2$ corresponds to a point in the vicinity of the point where the LSND and all-but-LSND regions in Fig. 4 first meet. From the curve in Fig. 5 we see that the improvement obtained by moving to the minimum at $\Delta\bar{m}_{21}^2 = 5 \times 10^{-4} \text{ eV}^2$ is only 0.5 units in χ^2 . We conclude that higher $\Delta\bar{m}_{21}^2$ values do not significantly affect the overall status of the CPT violating scenario.

IV. CONCLUSIONS

We have explored the possibility of explaining all the existing neutrino anomalies without enlarging the neutrino sector but allowing for CPT violation as described by the scenario in Fig. 1. In order to do so we have performed a compatibility test between the results of the oscillation analysis of the LSND on one side and all-but-LSND data on the other in the framework of $3\nu+3\bar{\nu}$ oscillations. Our main results are shown in Fig. 4. We find that the allowed regions for both data sets have no overlap at 3σ CL. Alternatively, using the so-called parameter goodness-of-fit our results imply that the probability for compatibility between both data sets within this scenario is only 7.5×10^{-4} .

The information most relevant to our conclusion comes from the atmospheric neutrino events. Our results show that, within the constraints imposed by solar and LBL neutrino data, and reactor anti-neutrino experiments, atmospheric data is precise enough to be sensitive to anti-neutrino oscillation parameters and cannot be described with oscillations with the wavelengths required in the CPT violating scenario.

Furthermore, the global oscillation data without LSND show no evidence for any CPT violation. An analysis of the all-but-LSND data set allowing for different mass and mixing parameters of neutrinos and anti-neutrinos gives a best fit point very close to perfect CPT conservation.

Acknowledgments

This work was supported in part by the National Science Foundation grant PHY0098527. M.C.G.-G. is also supported by Spanish Grants No FPA-2001-3031 and CTIDIB/2002/24. M.M. is supported by the Spanish grant BFM2002-00345, by the European Commission RTN network HPRN-CT-2000-00148, by the European Science Foundation Neutrino Astrophysics Network No 86, and by the Marie Curie contract HPMF-CT-2000-01008. T.S. is

supported by the “Sonderforschungsbereich 375-95 für Astro-Teilchenphysik” der Deutschen Forschungsgemeinschaft.

- [1] A. Aguilar *et al.* [LSND Collaboration], Phys. Rev. D **64**, 112007 (2001).
- [2] Q. R. Ahmad *et al.*, Phys. Rev. Lett. **87**, 071301 (2001); Q. R. Ahmad *et al.*, *ibid.* **89** 011301 (2002).
- [3] S. Fukuda *et al.* [Super-Kamiokande Collaboration], Phys. Lett. B **539**, 179 (2002).
- [4] B. T. Cleveland *et al.*, Astrophys. J. **496**, 505 (1998).
- [5] J. N. Abdurashitov *et al.*, J. Exp. Theor. Phys. **95**, 181 (2002).
- [6] GALLEX collaboration, W. Hampel *et al.*, Phys. Lett. B **447**, 127 (1999).
- [7] GNO collaboration, E. Bellotti, Nuclear Phys. B (Proc. Suppl.) **91**, 44 (2001).
- [8] M. Shiozawa, SuperKamiokande Coll., in *XXth International Conference on Neutrino Physics and Astrophysics*, Munich May 2002, (<http://neutrino2002.ph.tum.de>).
- [9] Y. Fukuda *et al.*, Phys. Lett. **B433**, (1998) 9; Phys. Lett. **B436**, (1998) 33; Phys. Lett. **B467**, (1999) 185; Phys. Rev. Lett. **82**, (1999) 2644.
- [10] M. Ambrosio *et al.*, MACRO Coll., Phys. Lett. B **517**, (2001) 59.
- [11] D. A. Petyt [SOUDAN-2 Collaboration], Nucl. Phys. Proc. Suppl. **110**, 349 (2002).
- [12] K. Eguchi *et al.* [KamLAND Collaboration], Phys. Rev. Lett. **90**, 021802 (2003).
- [13] H. Murayama and T. Yanagida, Phys. Lett. B **520**, 263 (2001).
- [14] G. Barenboim, L. Borissov, J. Lykken and A. Y. Smirnov, JHEP **0210**, 001 (2002).
- [15] J. N. Bahcall, M. C. Gonzalez-Garcia and C. Pena-Garay, JHEP **0207**, 054 (2002). M. Maltoni, T. Schwetz, M.A. Tortola and J.W.F. Valle, Phys. Rev. D **67**, 013011 (2003); V. Barger, D. Marfatia, K. Whisnant and B.P. Wood, Phys. Lett. **B 537** (2002) 179; P. Creminelli, G. Signorelli and A. Strumia, JHEP **05** (2001), 052; [hep-ph/0102234, see addendum 04/22/2002]; G.L. Fogli, E. Lisi, A. Marrone, D. Montanino and A. Palazzo, Phys. Rev. **D 66** (2002) 053010; A. Bandyopadhyay, S. Choubey, S. Goswami and D.P. Roy, Phys. Lett. **B 540** (2002) 14; P.C. de Holanda and A.Yu. Smirnov, Phys. Rev. D **66**, 113005 (2002).
- [16] G. Barenboim and J. Lykken, Phys. Lett. B **554**, 73 (2003).
- [17] G. Barenboim, L. Borissov and J. Lykken, hep-ph/0212116.
- [18] G. Barenboim, L. Borissov and J. Lykken, Phys. Lett. B **534**, 106 (2002).
- [19] M. Apollonio *et al.*, Phys. Lett. B **466**, 415 (1999).
- [20] Y. Declais *et al.*, Nucl. Phys. B **434**, 503 (1995).
- [21] A. Strumia, Phys. Lett. B **539**, 91 (2002), hep-ph/0201134.
- [22] S. Skadhauge, Nucl. Phys. B **639**, 281 (2002).
- [23] See for example, I. Mocioiu and M. Pospelov, Phys. Lett. B **534**, 114 (2002); A. De Gouvea, Phys. Rev. D **66** (2002) 076005; O.W. Greenberg, Phys. Rev. Lett. **89**, 231602 (2002).
- [24] V.A. Kostelecky, ed., *CPT and Lorentz Symmetry II*, World Scientific, Singapore, 2002.

- [25] J. N. Bahcall, V. Barger and D. Marfatia, Phys. Lett. B **534**, 120 (2002).
- [26] B. Pontecorvo, J. Exptl. Theoret. Phys. **33**, 549 (1957) [Sov. Phys. JETP **6**, 429 (1958)]; Z. Maki, M. Nakagawa and S. Sakata, Prog. Theo. Phys. **28**, (1962) 870 ; M. Kobayashi and T. Maskawa, Prog. Theor. Phys. **49**, (1973) 652.
- [27] Particle Data Group, D. E. Groom *et al.*, Eur. Phys. J. **C15**, (2000) 1.
- [28] J. N. Bahcall, M. C. Gonzalez-Garcia and C. Pena-Garay, JHEP **0302**, 009 (2003); M. Maltoni, T. Schwetz and J. W. Valle, Phys. Rev. D **67**, 093003 (2003).
- [29] W. Grimus and T. Schwetz, Eur. Phys. J. C **20**, 1 (2001).
- [30] E. D. Church, K. Eitel, G. B. Mills and M. Steidl, Phys. Rev. D **66** (2002) 013001.
- [31] M. H. Ahn *et al.*, Phys. Rev. Lett. **90**, 041801 (2003).
- [32] J. N. Bahcall, M. H. Pinsonneault, and S. Basu, Astrophys. J. **555**, 990 (2001).
- [33] M. C. Gonzalez-Garcia and C. Pena-Garay, hep-ph/0306001.
- [34] A.M. Dziewonski and D.L. Anderson, Phys. Earth Planet. Inter. **25**, (1981) 297.
- [35] N. Fornengo, M. C. Gonzalez-Garcia and J. W. Valle, Nucl. Phys. B **580**, 58 (2000); M. C. Gonzalez-Garcia, H. Nunokawa, O. L. Peres and J.W. Valle, Nucl. Phys. B **543**, 3 (1999); M. C. Gonzalez-Garcia, H. Nunokawa, O. L. Peres, T. Stanev and J. W. Valle, Phys. Rev. D **58**, 033004 (1998); M. C. Gonzalez-Garcia, M. Maltoni, C. Pena-Garay and J. W. Valle, Phys. Rev. D **63**, 033005 (2001).
- [36] B. Armbruster *et al.*, KARMEN Coll., Phys. Rev. D **65** (2002) 112001.
- [37] S. M. Bilenky, M. Freund, M. Lindner, T. Ohlsson and W. Winter, Phys. Rev. D **65** (2002) 073024.
- [38] M. Maltoni, T. Schwetz, M. A. Tortola and J. W. Valle, Nucl. Phys. B **643**, 321 (2002).
- [39] M. Maltoni and T. Schwetz, hep-ph/0304176.
- [40] O. L. Peres and A. Y. Smirnov, Phys. Lett. B **456**, 204 (1999); Nucl. Phys. Proc. Suppl. **110** (2002).
- [41] M. C. Gonzalez-Garcia and M. Maltoni, Eur. Phys. J. C **26**, 417 (2003).